Purdue University
Purdue e-Pubs

CTRC Research Publications | Cooling Technologies Research Center

2019

Supplemental - Three-Dimensional Liquid-Vapor Interface Reconstruction from High-Speed Stereo Images during Pool Boiling

C. Mira-Hernandez
Purdue University

J. A. Weibel
Purdue University

P. P. Vlachos
Purdue University

S. V. Garimella
Purdue University

Follow this and additional works at: https://docs.lib.purdue.edu/coolingpubs

Mira-Hernandez, C.; Weibel, J. A.; Vlachos, P. P.; and Garimella, S. V., "Supplemental - Three-Dimensional Liquid-Vapor Interface Reconstruction from High-Speed Stereo Images during Pool Boiling" (2019). *CTRC Research Publications.* Paper 343.
https://docs.lib.purdue.edu/coolingpubs/343

This document has been made available through Purdue e-Pubs, a service of the Purdue University Libraries. Please contact epubs@purdue.edu for additional information.

Three-dimensional liquid-vapor interface reconstruction from high-speed stereo images during pool boiling

Supplementary information

Carolina Mira-Hernández, Justin A. Weibel, Pavlos P. Vlachos, Suresh V. Garimella
School of Mechanical Engineering, Purdue University
585 Purdue Mall, West Lafayette, IN 47907 USA

Validation of liquid-vapor interface reconstruction technique

The liquid-vapor interface reconstruction technique is validated by imaging samples of known geometry. The samples are thin-walled, hollow, transparent and smooth plastic spheres (diameters of 30, 40 and 50 mm) with light-gray speckle pattern painted on the exterior surface. The use of transparent and smooth plastic samples mimics the transparency and specular reflectivity of liquid-vapor interfaces, which deviate from the typical opaque and diffuse reflecting objects that are used in standard stereo surface reconstruction, and can induce ambiguity during the correspondence search. Also, the transparency of the samples replicates the non-uniform illumination characteristics of real vapor bubbles that result from the lensing effect of curved objects immersed in a medium of higher optical density. The speckle pattern is widely used in the digital image correlation community and provides randomly distributed features of different sizes that are favorable for the correspondence search. The characteristics of the actual liquid-vapor interfaces that form during boiling are extremely difficult to replicate in a controlled and representative manner; however, the texture captured in the acquired images for vapor structures generally appear to have randomness in shape and orientation. The spherical shape of the samples allows evaluation of the effects of the disparity gradient on the correspondence search due to distortion of features between the left and right views. A spherical surface covers the entire range of orientations of surface patches with respect to the camera configuration, which is critical because the magnitude of the disparity gradient increases with inclination. Disparity gradients also intensify with increasing curvature; hence, samples of different radii are considered in the validation.

The validation samples are place inside the test section filled with deionized water at room temperature. Stereoscopic images of the samples are taken using the same camera configuration as for the images acquired during the pool boiling experiments. Figure S1a presents the left grayscale images of the validation samples. The reconstruction of the front surface of the validation samples is performed following the same general process as for the pool boiling images. The only differences are the manual creation of the masks due to the simple geometry, and the use of single-frame correlation because the validation samples are static. The parameters for feature extraction, corresponding search and

reconstruction filtering are identical as for the pool boiling images. For estimating the error in the reconstruction results, the location of the center of each sample is found by fitting a spherical surface of fixed known diameter to the reconstructed surface. To facilitate the interpretation of the results, the reconstructed surfaces are translated to make the coordinates origin coincident with the center of the samples. Figure S1b presents the resulting reconstructions for the validation samples with dimensions normalized by the sample radius. The surface reconstructions exhibit some discontinuities on the periphery due to reduced contrast in the captured features and significant distortion of the features between views. Discontinuities are also observed near the center of each reconstruction, where the reconstruction process is affected by ambiguity between the features on the front surface and features on the rear surface and by the distorted image of the rear illumination window that is generated due to the sample lensing effect; similar discontinuities are observed in the reconstruction of real vapor bubbles. The error is computed as the difference between the sample radius and the distance of the reconstructed points to the sample center. Figure S1c presents the reconstruction error map normalized by the validation sample radius. The reconstruction error is low, aside from outliers near the previously mentioned discontinuities. Figure S1d presents the probability distribution of the normalized error for the three samples. The normalized error distribution becomes narrower with increasing sample size, which is a consequence of the error normalization. Standard bounds for the normalized error, *i.e.* 68.5% coverage, are 0.024, 0.016, 0.014, which correspond to dimensional standard bounds of 0.36 mm, 0.32 mm and 0.35 mm for samples diameters of 30, 40 and 50 mm respectively.

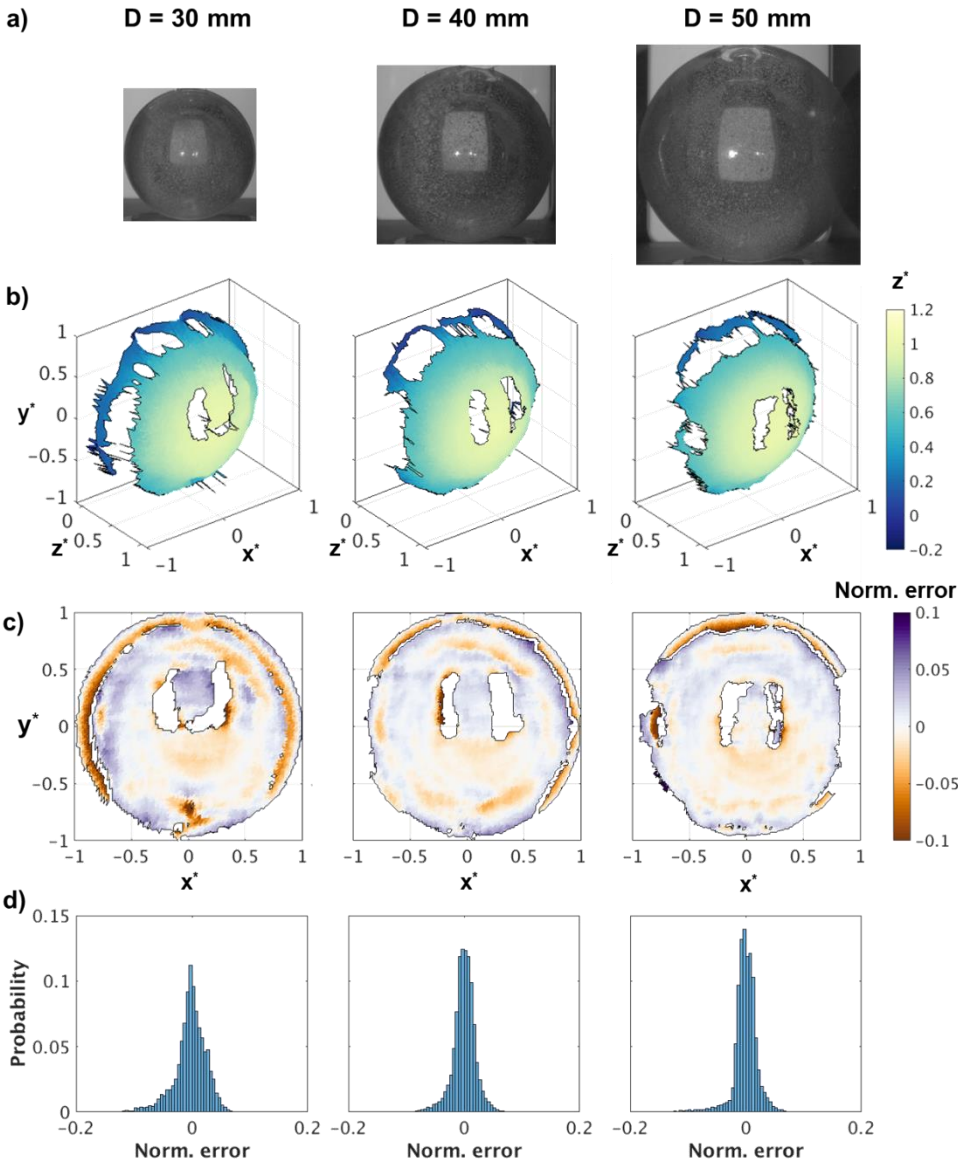

Figure S1. Validation samples (a) original left grayscale image, (b) reconstructed surface and depth map, (c) normalized error map, and (d) normalized error distribution.